doi:10.1093/brain/awz104 BRAIN 2019: 142; 1690–1700 | 1690

BRAIN
A JOURNAL OF NEUROLOGY

Temporal evolution of microglia and α-synuclein accumulation following foetal grafting in Parkinson's disease

C. Warren Olanow,[1,2] Mari Savolainen,[3] Yaping Chu,[3] Glenda M. Halliday[4] and Jeffrey H. Kordower[3]

We observed Lewy pathology in healthy embryonic dopamine neurons implanted into the striatum of patients with advanced Parkinson's disease. In the present study we examined the temporal relationship between the presence of inflammation with activated microglia and the emergence of α-synuclein pathology. Inflammation with activated microglia was observed in all grafts and at all time points examined between 18 months and 16 years as determined by both CD45 and TMEM119 staining. In contrast, α-synuclein was not detected at 18 months, only diffuse monomeric α-synuclein staining was observed at 4 years, and α-synuclein aggregates were not observed until 14–16 years after transplantation. Thus, there is evidence of inflammation and microglial activation in graft deposits long before the accumulation of α-synuclein pathology in implanted dopamine neurons. These observations raise the possibility that microglial activation contributes to the development of α-synuclein pathology, and supports the concept that microglia play an integral role in the propagation and spread of α-synuclein pathology.

1 Department of Neurology and Department of Neuroscience, Mount Sinai School of Medicine, New York, NY 10029, USA
2 Clintrex Research Inc, Sarasota, Florida 34236, USA
3 Department of Neurological Sciences, Rush University Medical Center, Chicago Illinois 60612, USA
4 Neuroscience Research Australia and Faculty of Medicine, University of New South Wales, Sydney, New South Wales 2031, Australia

Correspondence to: C. Warren Olanow MD, FRCPC
Department of Neurology and Department of Neuroscience, Mount Sinai School of Medicine, NY, USA
E-mail: cwolanow@gmail.com

Keywords: Parkinson's disease; α-synuclein; microglia

Introduction

Previously, we described robust survival of healthy appearing dopamine neurons 18 months following transplantation of foetal mesencephalic tissue into the striatum of patients with advanced Parkinson's disease (Kordower *et al.*, 1995, 1996; Olanow *et al.*, 2003). In these studies, embryonic dopamine neurons derived from either one or four donors per side, were implanted into the post-commissural putamen bilaterally using eight needle tracts per side and four deposits per tract. Cell counting demonstrated 80 000–120 000 healthy appearing tyrosine hydroxylase (TH)-positive neurons in each putamen, with extensive organotypic innervation of the host striatum. However, two double-blind studies failed to meet their primary end-points (Freed *et al.*, 2001; Olanow *et al.*, 2003), and the procedure was complicated by the development of often disabling graft-induced dyskinesias that persisted despite stopping

Received October 15, 2018. Revised February 12, 2019. Accepted February 22, 2019. Advance Access publication May 5, 2019
© The Author(s) (2019). Published by Oxford University Press on behalf of the Guarantors of Brain. All rights reserved.
For Permissions, please email: journals.permissions@oup.com

Downloaded from https://academic.oup.com/brain/article/142/6/1690/5485812 by guest on 20 April 2024

levodopa (Olanow *et al.*, 2009*a*). Based on these results and other considerations, we discontinued our transplant programme (Olanow *et al.*, 2009*b*).

Approximately 14 years following the initial transplant procedure, our group and others co-discovered Lewy pathology in cell bodies and axons of the embryonic dopamine neurons that had been implanted into the striatum of these advanced Parkinson's disease patients (Kordower *et al.*, 2008*a*, *b*; Li *et al.*, 2008). The inclusions stained positively for α-synuclein, ubiquitin, and thioflavin S, and were proteinase K resistant, indicating protein misfolding with beta-sheet formation and aggregation. The inclusions in the implanted dopamine neurons were morphologically identical to Lewy bodies seen in neurons of the host substantia nigra pars compacta (SNc). Importantly, the implanted cells were derived from multiple unrelated donors, and inclusions were seen in all deposit sites in each patient, and at a time when Lewy pathology is virtually never seen under normal circumstances. We speculated that Lewy pathology developed in the healthy implanted dopamine neurons as a result of their being placed into a Parkinson's disease milieu, and represented transmission of misfolded α-synuclein from host Parkinson's disease-affected neurons in a prion-like manner (Olanow and Prusiner, 2009). Indeed, similar results have been seen in experimental models (Kordower *et al.*, 2011; Angot *et al.*, 2012). In subsequent years, a body of experimental evidence has been developed supporting the prion hypothesis in Parkinson's disease (Olanow and Brundin, 2013). Fundamental to the prion theory is the concept of permissive templating, whereby misfolded proteins promote misfolding of the native unfolded proteins, thereby sustaining an infectious chain reaction.

The mechanism whereby Lewy pathology develops in implanted dopamine neurons remains unknown. Recent experimental studies suggest that immune activation of microglia with cytokine release might play a critical role in promoting α-synuclein misfolding, and in the spread of misfolded α-synuclein (Bassil *et al.*, 2016; Sampson *et al.*, 2016; Wang *et al.*, 2016). In this regard, it is noteworthy that in our initial studies we observed robust CD45 cell staining surrounding graft deposits indicative of an inflammatory reaction, with some cells displaying a morphology suggestive of activated microglia (Kordower *et al.*, 1997; Olanow *et al.*, 2003). However, our initial studies were performed prior to the discovery of α-synuclein mutations in Parkinson's disease (Polymeropoulos *et al.*, 1997), and the appreciation that this protein is a major component of Lewy pathology in sporadic cases (Spillantini *et al.*, 1997). In the present study, we examined the evolution of α-synuclein accumulation and aggregation in graft deposits, and its temporal relationship with inflammation and microglial activation. We were able to examine brains derived from six transplanted Parkinson's disease patients who died at 18 months ($n = 1$ patient), 4 years ($n = 2$ patients), 14 years ($n = 2$ patients), and 16 years ($n = 1$ patient) following the procedure. This is the largest post-mortem sample of transplanted brains reported to date and is of particular interest in view of the increasing evidence suggesting that activated microglia might play a role in promoting the misfolding, seeding, aggregation, and spread of α-synuclein in Parkinson's disease as part of a prion-like process.

Materials and methods

General immunohistochemistry procedures

Endogenous peroxidase-containing elements were eliminated by 20 min incubation in 0.1 M sodium periodate, and background staining was blocked by 1 h incubation in a solution containing either 2% bovine serum albumin or 5% horse serum. Series of sections through the rostrocaudal striatum and SNc were immunostained with primary antibodies (see below) overnight at room temperature. After six washes, sections were sequentially incubated for 1 h in biotinylated secondary antibody (1:200; Vector) followed by Elite® avidin–biotin complex (1:500; Vector) for 75 min. The immunohistochemical reaction was completed with 0.05% 3, 3′-diaminobenzidine (DAB) and 0.005% H_2O_2. Sections were mounted on gelatin-coated slides, dehydrated through graded alcohol, cleared in xylene, and coverslipped with Cytoseal™ (Richard-Allan Scientific™).

TH, dopamine transporter and ubiquitin

The immunoperoxidase labelling method was used to perform TH, dopamine transporter (DAT) and ubiquitin immunohistochemistry as described previously (Chu and Kordower, 2007; Kordower *et al.*, 2008*a*, *b*).

α-Synuclein

Separate series of sections were incubated with antibodies directed against total α-synuclein (LB509) and phosphoserine 129 α-synuclein (ab51253, Abcam, 1:1000) overnight at room temperature, as previously described (Chu and Kordower, 2007). We used proteinase K digestion to determine whether the α-synuclein was soluble (non-aggregated) or insoluble (aggregated). Sections were mounted onto gelatin-coated slides and dried for at least 8 h at 55°C. After wetting with TBS-T (10 mM Tris–HCl pH 7.8, 100 mM NaCl, 0.05% Tween-20), the sections were digested with 50 μg/ml proteinase K (Invitrogen) in TBS-T for 3 h at 55°C. The sections were fixed with 4% paraformaldehyde for 10 min. After several washes, the sections were then processed for α-synuclein immunostaining as described above.

CD45

CD45 staining was carried out to assess inflammation and inflammatory cells, including macrophages and microglia (Cosenza-Nashat *et al.*, 2006; Bennett *et al.*, 2016). Sections were incubated with primary antibody, mouse anti-CD45 (1:500, BD Biosciences) overnight at room temperature (Kordower *et al.*, 1997) and processed as described above.

Downloaded from https://academic.oup.com/brain/article/142/6/1690/5485812 by guest on 20 April 2024

TMEM119

Transmembrane protein 119 (TMEM119) staining was used to more specifically assess for the presence of brain resident microglia (Bennett *et al.*, 2016; Li and Barres, 2018; Lopez-Atalaya *et al.*, 2018). Tissue sections from all cases were immunostained with TMEM119 antibody (1:500, Abcam) and processed immunohistochemically as described above.

Stereological quantification

TH neurons

Stereological estimates of grafted TH-immunoreactive neurons were carried out for every transplant site using an unbiased sampling scheme and the optical fractionator procedure (Kordower *et al.*, 2017). We evaluated grafted neurons in ~14–20 equi-spaced sections throughout the striatum on each side. The sectional sampling fraction (ssf) was 1/0.055. The distance between sections was ~720 µm. Each graft was outlined according to the pattern of TH staining using a ×4 objective. A systematic sample of the area occupied by grafts was made from a random starting point (StereoInvestigator v10.40 software; Micro BrightField, Colchester, VT). Counts were made at regular predetermined intervals (x = 313 µm, y = 313 µm), and a counting frame (70 × 70 µm = 4900 µm^2) was superimposed on images obtained from tissue sections. The area sampling fraction (asf) was 1/0.05. These sections were then analysed using a 60× Planapo oil immersion objective with a 1.4 numerical aperture. The section thickness was empirically determined. Briefly, as the top of the section was first brought into focus, the stage was zeroed at the z-axis by software. The stage then stepped through the z-axis until the bottom of the section was in focus. Section thickness averaged 16.2 ± 2.3 µm in the striatum. The dissector height (counting frame thickness) was 10 µm. This method allowed for 2-µm top guard zones and at least 2-µm bottom guard zones. The thickness sampling fraction (tsf) was 1/0.61. Care was taken to ensure that the top and bottom forbidden planes were never included in the cell counting. The total number of TH-immunoreactive, phosphorylated α-synuclein-immunoreactive, and neuromelanin-laden neurons within the graft were calculated separately using the following formula:

$$N = \sum Q - \cdot \frac{1}{ssf} \cdot \frac{1}{asf} \cdot \frac{1}{tsf} \quad (1)$$

where ΣQ was the total number of raw counts (West *et al.*, 1991). The coefficients of error (CE) were calculated according to the procedure of Gunderson and colleagues as estimates of precision (Chu and Kordower, 2007; Kordower *et al.*, 2017). The CE values were 0.08 in left and 0.07 in right striatal grafts (Schmitz and Hof, 2005).

CD45 and TMEM119 immunoreactivities

CD45 (leucocyte common antigen) is an essential regulator of antigen receptor signalling and is present on haematopoietic cells, such as leucocytes and macrophages, as well as brain microglia. TMEM119 is a transmembrane protein that is specific for brain resident microglia (Bennett *et al.*, 2016; Lopez-Atalaya *et al.*, 2018). Semi-quantitative optical density analyses were carried out to assess CD45 and TMEM119 immunoreactivities in foetal tissue graft deposit sites. All assessments were made in a blinded fashion using three to five sections per case. Optical density was measured from an area within the transplant region and from an area with a similar volume outside of the graft region in transplanted patients; similar volumes within the caudate nucleus/putamen were also analysed in ungrafted Parkinson's disease controls and normal controls. Scion Image software was used for the measurement and mean optical density was calculated for each case. Statistical analysis to compare the overall CD45 and TMEM119 optical densities in graft regions of transplanted patients and areas outside of the graft was performed using GraphPad Prism 7.02 software (La Jolla, CA, USA). Paired Student's t-test was used.

Data availability

All data will be made available upon request.

Results

Neuronal TH expression in graft deposits

The number of surviving grafted dopamine neurons per putamen was estimated in cases where sufficient tissue was available (Table 1). Neuronal survival was relatively robust in each case, albeit with substantial variability. Interestingly, while receiving an identical number of donors, our shortest surviving case (18 months post-grafting) had ~100 000 surviving dopamine neurons per side (Kordower *et al.*, 1995), while our case with the longest survival (16 years post-transplantion) had ~300 000 surviving dopamine cells on each side (Kordower *et al.*, 2017). In each case, TH-positive grafted neurons reinnervated the striatum in an organotypic manner with a normal-appearing patch-matrix pattern and synaptic connectivity. Individual TH-positive cells displayed a morphological appearance typical of mesencephalic dopamine neurons. The breadth and density of TH innervation was relatively robust and similar in cases from 18 months to 14 years post-grafting. However, the 16-year post-graft case had significantly greater graft survival with TH reinnervation of the entire putamen at a level approximating that seen in normal age-matched controls, even though grafts were only placed into the post-commissural putamen. In addition, in all cases, TH immunoreactive fibres were seen traversing the internal capsule to reach the caudate nucleus. Nonetheless, in both the 14- and 16-year post-grafted cases we observed functional impairment of TH immunoreactive neurons as evidenced by a marked reduction in DAT (Kordower *et al.*, 2008*a*, *b*). These changes were not noted in the 18-month and 4-year post-transplantation cases suggesting a time-dependent loss of expression of dopamine markers.

Downloaded from https://academic.oup.com/brain/article/142/6/1690/5485812 by guest on 20 April 2024

Table 1 Relative profiles of TH+ cells, microglia and α-synuclein in the different cases

Case (post grafting)	TH cells (per putamen)	Microglia	α-Synuclein		Thioflavin-S
			Diffuse	Aggregated	
18 months	105 033	+ + +	-	-	-
4 years	45 108	n/a	+	-	-
4 years	75 508	+ + +	+	-	-
14 years	73 451	n/a	-	+ +	+ +
14 years	58 941	+ + +	-	+ +	+ +
16 years	308 558	+ + +	-	+ + +	+ +

n/a = not available.
– = undetectable; + = mild; ++ = moderate; +++ = severe.

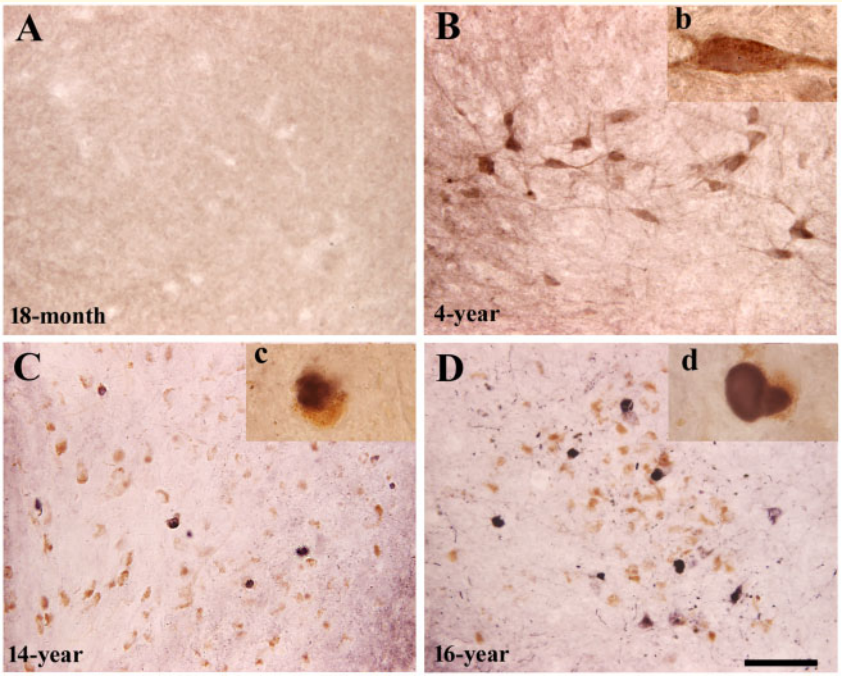

Figure 1 Time-dependent progression of α-synuclein accumulation and aggregation in foetal dopamine nigral grafts. Sections through the graft were stained for Ser129 phospho-synuclein. Scale bar = 100 μm (**A**–**D**); 20 μm (**a**–**d**).

Pattern of α-synuclein accumulation and distribution

To assess the presence and distribution of α-synuclein pathology within foetal tissue graft deposits, brain sections from each of our cases were immunostained with antibodies directed against total α-synuclein (LB509) and phosphorylated α-synuclein (Ser129-phosphorylated α-synuclein) (Fig. 1). In the 18-month post-surgical case, no α-synuclein immunoreactivity was detected in the grafted cells with either antibody. In both of the 4-year cases, diffuse staining of monomeric, proteinase K digestible, α-synuclein was seen throughout the cytosol of a few implanted cells close to the graft margins. There was no immunostaining for Ser129 phosphorylated α-synuclein or thioflavin S. In the older grafts (14 and 16 years post-transplantation), there was abundant staining for Ser129 phosphorylated α-synuclein inclusions in cell bodies and neurites that were proteinase K resistant. Ser129 α-synuclein positive inclusions were noted in ~5–30% of TH-positive grafted cells, with greater numbers in the 16-year than in the two 14-year cases. The 16-year post-graft case also had the most extensive Lewy neuritic pathology, involving fibres within the graft as well as within the host striatum. In both the 14- and 16-year post-graft cases, α-synuclein aggregates also stained positively for ubiquitin and thioflavin S indicating the presence of misfolded protein with beta-pleated sheet formation. In these older (14- and 16-year) grafts, less monomeric soluble α-synuclein staining was visible as aggregate

Downloaded from https://academic.oup.com/brain/article/142/6/1690/5485812 by guest on 20 April 2024

accumulation increased. These data suggest that within grafted embryonic neurons, there is a gradual accumulation of soluble α-synuclein that develops over 4 years post-transplantation and misfolded/aggregated α-synuclein that evolves over the course of approximately the next decade.

Pattern of CD45-labelled cells

To analyse inflammation in graft regions, brain sections from transplanted cases as well as from two non-transplanted Parkinson's disease patients and two normal age-matched controls were stained with CD45 (leucocyte common antigen) antibody to identify inflammation in the region of graft deposits. In normal brain, expression of CD45 is low, but when microglia are activated, CD45 expression is markedly upregulated and cells assume characteristic morphologies (Cosenza *et al.*, 2002; David and Kroner, 2011). However, this antibody is relatively non-specific and recognizes infiltrating lymphocytes and macrophages as well as activate microglia. In the four transplanted cases where tissue was available for analysis (18 months, 4 years, 14 years, and 16 years post-transplantation), there was a significant increase in CD45-positive cells in each of the grafted areas in comparison to non-grafted regions of the putamen, and in comparison to the putamen of non-transplanted Parkinson's disease patients and age-matched controls (Fig. 2). At 18 months, CD45 stained cells were round and ramified in morphology. The round cells displayed dark staining without processes suggesting that these cells were likely to be lymphocytes or infiltrating macrophages. The ramified cells exhibited light staining with more processes as compared to what was observed in the non-grafted putamen. In all of the older grafts (Fig. 2), dark stained CD45-positive cells with abundant short and large processes continued to be observed, but round cells suggestive of lymphocytes were no longer detected. The CD45-positive cells in non-grafted regions of the putamen were markedly fewer in number, and displayed lighter staining and longer and finer processes. In the grafts that were 18 months and 4 years post-transplantation, CD45-positive cells were somewhat heterogeneous with some areas relatively devoid of cells, whereas CD45-positive cells were more evenly distributed throughout the implant sites in the 14- and 16-year grafts. In the 18-month-old graft, CD45-positive cells were also observed around blood vessels near the grafted sites suggesting the possibility of either ongoing infiltration into the brain of CD45-positive inflammatory cells or greater activation and accumulation of immune activated cells at these sites (Fig. 3). In the older grafts, the cell morphology and increased CD45 expression was more consistent and restricted to the graft regions. Quantitative optical density measurements are shown in Fig. 2, and demonstrate significant increases in grafted regions of each transplanted patient in comparison to non-grafted regions in these same patients, and in comparison to comparable regions of the putamen in Parkinson's disease and control subjects who had not undergone a transplant procedure.

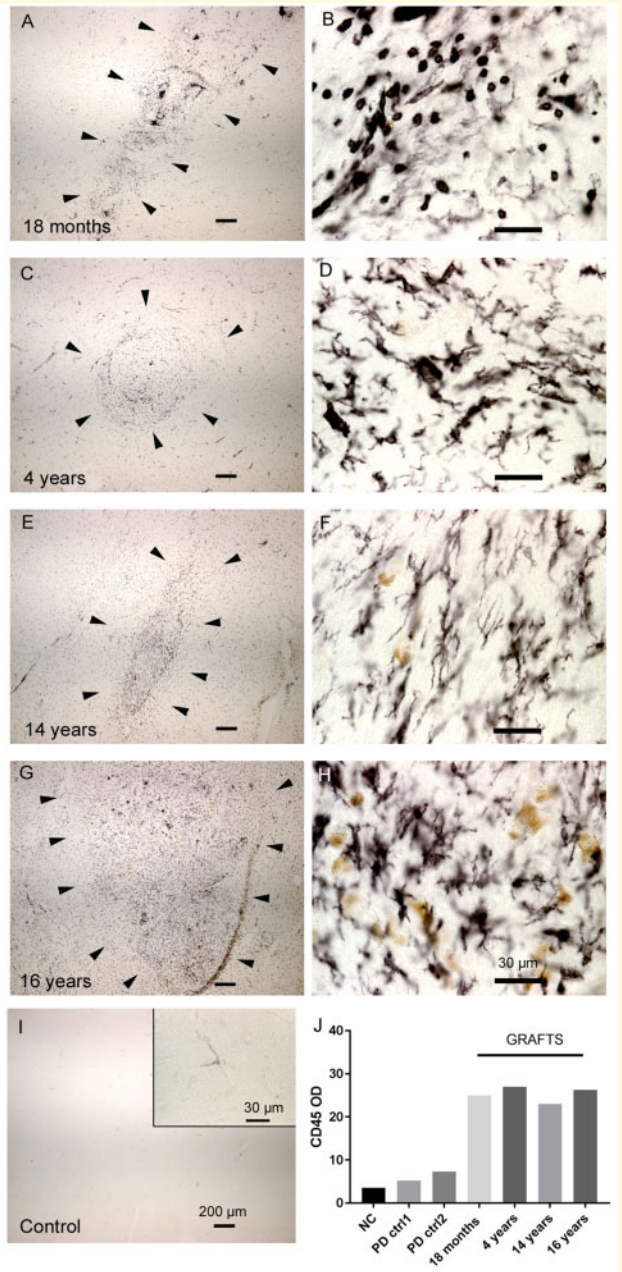

Figure 2 Qualitative and quantitative evidence for increased CD45 immunoreactivity was observed in grafted regions of the striatum at all time points examined. Representative low and high power examples are provided from the cases at 18 months (**A** and **B**), 4 years (**C** and **D**), 14 years (**E** and **F**) and 16 years (**G** and **H**) after transplantation and (**I**) an age-matched control. (**J**) Mean optical density (OD) measures of CD45 immunostaining was calculated for graft regions and comparable regions of the putamen of Parkinson's disease and controls. Data are presented as mean optical density in grafted versus non-grafted controls ($P < 0.0002$). Scale bar = 200 μm (**A**, **C**, **E**, **G** and **I**); 30 μm (**B**, **D**, **F**, **H** and inset **I**). NC = normal control; PD = Parkinson's disease.

Downloaded from https://academic.oup.com/brain/article/142/6/1690/5485812 by guest on 20 April 2024

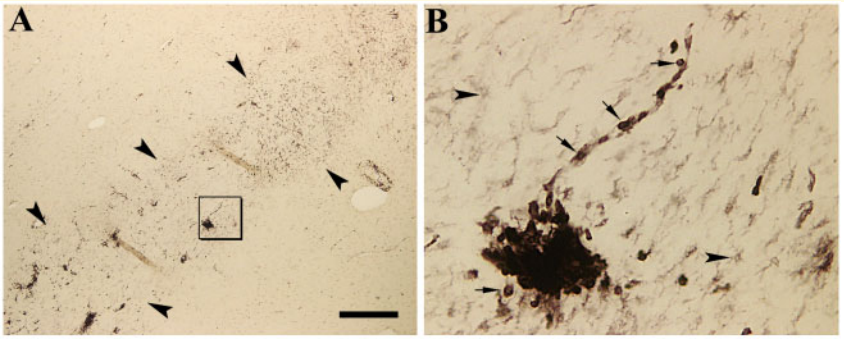

Figure 3 Low (A) and high power (B) photomicrographs from grafted region of 18 month graft illustrating CD45 immunoreactivity. Intense CD45-labelled inflammatory cells were observed within graft (arrowheads; **A**). Boxed area in **A** is enlarged in **B** showing two types of CD45-positive cells in graft: dark stained round cells with absent processes (arrows; **B**) associated with blood vessels within the graft, and light stained small cells with present processes (arrowheads; **B**) distributed either in grafted region or non-grafted putamen. Scale bars = 400 μm (**A**); 40 μm (**B**).

Pattern of TMEM119-labelled cells

To characterize the inflammatory cells that accumulate in grafted regions, brain tissues were immunostained with a TMEM119 antibody, which stains for a cell surface protein specific to brain resident microglia (Bennett *et al.*, 2016). TMEM119-positive cells displayed ramified morphological features in all brain areas (Fig. 4). TMEM119 staining in grafted patients was much more pronounced than in non-grafted Parkinson's disease patients or control subjects. Robust dark and dense TMEM119 staining was observed in all grafted regions at all time points examined, with immunoreactivity mainly seen in processes (Fig. 4). TMEM119-labelled cells had enlarged cell bodies with both short and large processes that displayed a bushy-like (non-amoeboid) morphology. In contrast, in non-grafted regions of the putamen, TMEM119-positive cells displayed small cell bodies with long ramified processes (Fig. 5), similar to those seen in patients with Parkinson's disease who had not undergone a transplant procedure, and greater than in healthy controls. The density of TMEM119-positive cells in 18-month-old grafts was somewhat less than in the 4–16-year-old grafts. Further, in the older grafts, the TMEM119-positive cells accumulated around the periphery of the graft with only a few TMEM119-positive cells in the centre area, similar to the distribution pattern observed for grafted dopaminergic neurons.

Quantitative optical density measures (Fig. 4E) confirmed that there was a significant increase in TMEM119 immunoreactivity in grafted regions of each transplanted patient in comparison to non-grafted regions of the putamen, and in comparison to comparable regions of the putamen of Parkinson's disease subjects who had not undergone a transplant procedure and normal age-matched controls.

Discussion

We demonstrate that pathological α-synuclein aggregation in embryonic dopamine neurons that have been implanted into the striatum of patients with advanced Parkinson's disease develops gradually over the course of ∼14–16 years. No α-synuclein staining was detected in any of the grafted neurons in any of the 64 deposit sites in the single case examined at 18 months post-transplantation. In the two cases at 4 years, there was a diffuse homogeneous pattern of staining for α-synuclein in transplanted dopamine neurons that was proteinase K digestible and was not associated with staining for thioflavin S. These findings are consistent with the accumulation of soluble α-synuclein, but without misfolding or aggregate formation. In the two cases at 14 years and the one case at 16 years post-transplantation, there was prominent α-synuclein aggregate formation in dopamine nerve cells and terminals in all deposit sites, affecting ∼5–30% of the implanted dopaminergic cells. At these time points, the aggregates were proteinase K resistant, stained positively for ubiquitin and thioflavin S, and were indistinguishable from Lewy bodies in the SNc neurons of these same patients as we have previously reported (Kordower *et al.*, 2008*a*, *b*, 2017). These data suggest that in grafted, dopaminergic neurons placed into the Parkinson's disease brain, there is a slow, gradual, decade-long accumulation of misfolded α-synuclein. In this regard it should be noted that α-synuclein aggregates are virtually never seen in dopamine neurons of this age.

In contrast, staining for inflammation (CD45) and specifically for activated microglia (TMEM119) was markedly increased in all graft sites in comparison to non-grafted regions of the putamen in transplanted patients, and in comparison to all regions of the putamen in non-grafted Parkinson's disease patients and healthy controls (Fig. 2). This staining pattern was observed at all time points exam-

Downloaded from https://academic.oup.com/brain/article/142/6/1690/5485812 by guest on 20 April 2024

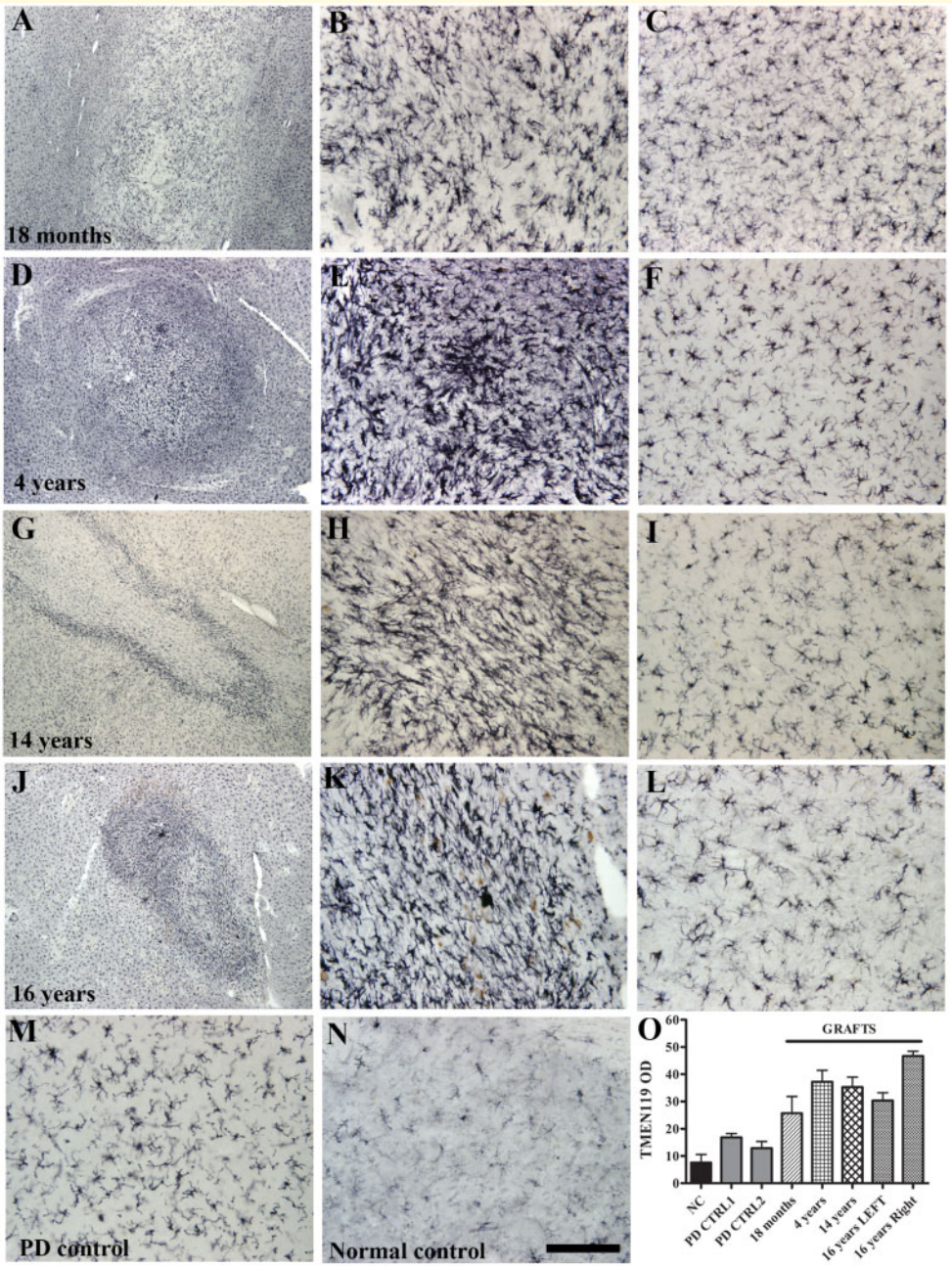

Figure 4 Photomicrographs showing TMEM119 immunoreactivity. Photomicrographs from grafted regions (**A**, **B**, **D**, **F**, **G**, **H**, **J** and **K**), putamenal area remote from graft deposits (**C**, **F**, **I** and **L**), Parkinson's disease control putamen (**M**), and control (**N**), illustrating TMEM119 immunoreactivity. The grafted samples were collected from 18 month (**A** and **B**), 4 year (**D** and **E**), 14 year (**G** and **H**), and 16 year (**J** and **K**) time points after transplantation. Note that intense TMEM119 labelled microglia were observed within grafts at all time points examined as compared with putamenal area remote from graft deposits and Parkinson's disease patients who did not undergo a transplant procedure. Scale bar = 100 μm in **N** (applies to **B**, **C**, **E**, **F**, **H**, **I**, **K**, **L** and **M**); 500 μm in **A**, **D**, **G** and **J**. Mean optical density (OD) of TMEM119 immunostaining was calculated for graft regions and comparable regions of the putamen of Parkinson's disease subjects and controls (**O**). Data are presented as mean optical density versus non-grafted controls ($P < 0.05$ to $P < 0.001$). NC = normal control; PD = Parkinson's disease.

ined (18 months to 16 years). CD45-positive staining and the appearance of the cells is indicative of inflammation, but could represent infiltrating peripheral macrophages particularly at 18 months. However, positive staining with TMEM19, which is a specific marker for brain resident microglia, indicates that the inflammation in graft regions is principally associated with activated microglia even at the 18-month time point. These findings contrast with α-synuclein staining, which was not detected at 18 months, and showed only diffuse soluble, non-aggregated α-synuclein

Downloaded from https://academic.oup.com/brain/article/142/6/1690/5485812 by guest on 20 April 2024

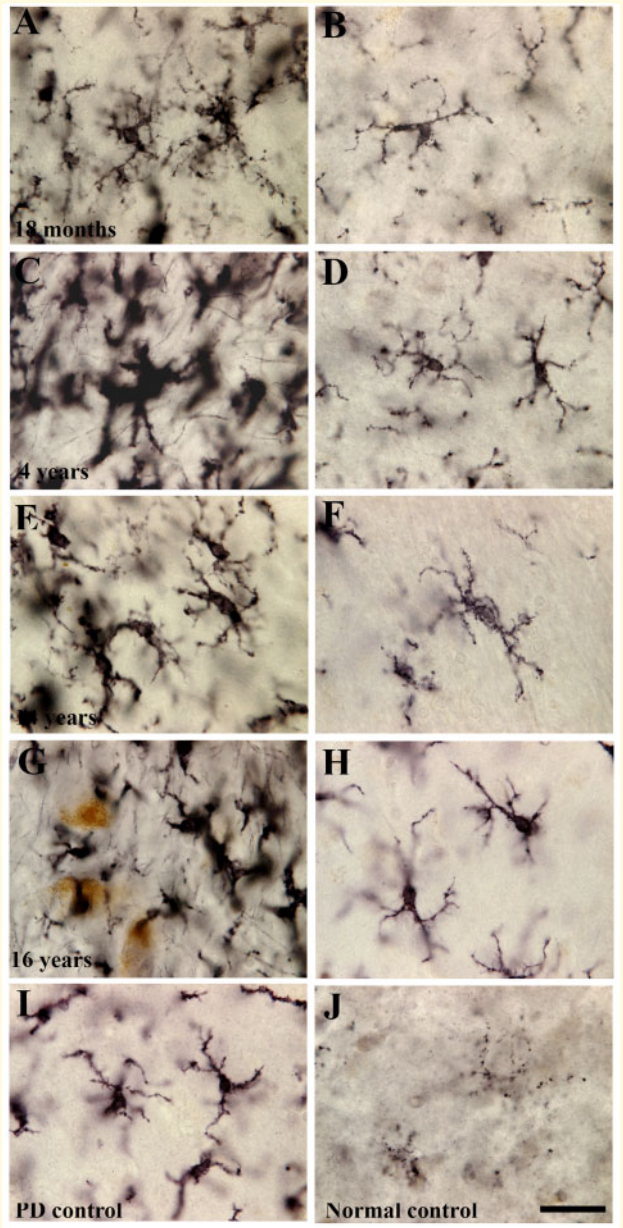

Figure 5 Photomicrographs showing morphological pattern of TMEM119-labelled microglia. High power photomicrographs from grafted regions (**A**, **C**, **E** and **G**), putamenal area remote from graft deposits (**B**, **D**, **F** and **H**), Parkinson's disease control (**I**), and normal control (**J**) illustrating morphological pattern of TMEM119-labelled microglia. The TMEM119-positive microglia inside grafts at all time points examined displayed dense swollen and short processes and enlarged cell bodies with bushy morphology (**A**, **C**, **E** and **G**). However, in putamen remote from grafts (**B**, **D**, **F** and **H**) and Parkinson's disease control (**I**), TMEM119 labelled small cell bodies and long ramified processes. In age-matched control (**J**), TMEM-positive microglia exhibited light stained cell bodies and fine ramified processes. Scale bar = 30 μm in **J** (applies to all).
PD = Parkinson's disease.

accumulation at 4 years post-transplantation. Ser129 phosphorylated α-synuclein immune-positive, proteinase K-resistant aggregates with thioflavin S-positive staining indicative of misfolded α-synuclein were not observed until the cases examined 14 and 16 years after transplantation. Thus, there is evidence of abundant and persistent inflammation and microglial activation in all graft deposit sites years before the accumulation of α-synuclein aggregates in implanted dopamine neurons.

Our data demonstrating that following dopamine cell transplantation, microglial activation is present many years prior to α-synuclein deposition and aggregation, raise the possibility that microglial activation might contribute to the development of α-synuclein pathology in the implanted dopamine neurons, and support the concept that activated microglia play an integral role in the propagation and spread of α-synuclein pathology (David and Kroner, 2011; Tomé *et al.*, 2013; Dzamko *et al.*, 2017; Valdinocci *et al.*, 2017). Recent studies have begun to shed light on how this might occur. Activated microglia secrete toxic cytokines such as caspase-1 and calpains, which metabolize and cleave α-synuclein at the C-terminus causing the protein to misfold and aggregate (Dufty *et al.*, 2007; Levesque *et al.*, 2010). In cell culture studies, menadione, which promotes caspase-1 activity, induces dose-dependent truncation and aggregation of α-synuclein (Angot *et al.*, 2012) that can be blocked by inhibiting caspase-1 with shRNAs or the caspase-1 inhibitor VX765. Importantly, studies in transgenic mice that overexpress α-synuclein show that VX765 prevents α-synuclein misfolding and aggregation, as well as degeneration of SNc dopamine neurons (Bassil *et al.*, 2016). Further, it has been demonstrated that activated microglia associated with the Parkinson's disease microbiome are critical for the spread of α-synuclein pathology to the CNS and the development of motor dysfunction in α-synuclein transgenic mice (Wang *et al.*, 2016). In these transgenic animals, antibiotic treatment, which suppresses the microbiome and the associated microglial activation, prevents α-synuclein transfer to the brain and the development of motor impairment. Subsequent gastric infusion of extracts derived from the microbiome of Parkinson's disease patients, but not from normal individuals, causes recurrence of microglial activation with the transfer of α-synuclein to the CNS and the development of motor deficits.

In our transplanted cases, microglial activation could have been initiated by an immune reaction due to the implantation of foreign tissue or by the surgical procedure itself. Indeed, we observed a prominent increase in CD45 cell staining surrounding blood vessels in the early grafted cases, suggesting the possibility of infiltrating macrophages from the periphery consequent to a surgically-induced disruption of the blood–brain barrier (Dudvarski *et al.*, 2016). It is also interesting to speculate that activated microglia could release toxic cytokines causing host α-synuclein to misfold and aggregate, and that pathological α-synuclein released from cells could be taken up by microglia causing them to become, or continue to be, activated, thus accounting for the continued presence of inflammation and the progressive α-synuclein

Downloaded from https://academic.oup.com/brain/article/142/6/1690/5485812 by guest on 20 April 2024

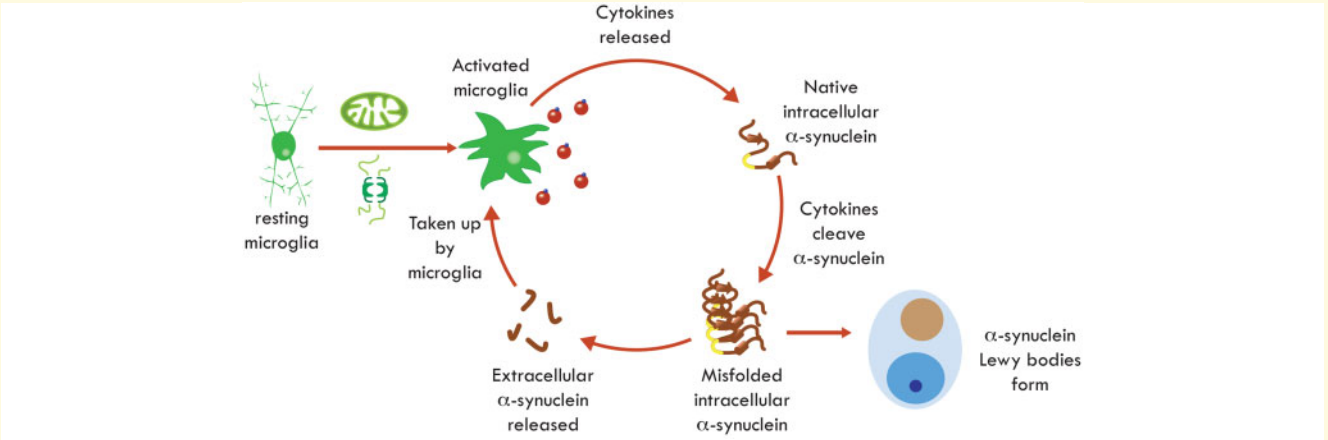

Figure 6 Schematic of the viscous cycle between inflammation and Lewy pathology. Schematic illustration demonstrating how a variety of factors including the implantation of foreign tissue could cause microglia to become activated and initiate a vicious cycle in which toxic cytokines cause native α-synuclein to misfold, and the uptake of misfolded α-synuclein causes microglia to become activated. In this scenario, microglia become activated and release toxic cytokines, which can metabolize and cleave native α-synuclein causing it to misfold, aggregate, and form pathological inclusions (Lewy pathology). Misfolded α-synuclein can be released from cells and taken up by microglia causing them to become activated with the release of toxic cytokines, thereby perpetuating the vicious cycle. The release of different toxic cytokines from microglia may cause α-synuclein to form and fold differently to cause the known diversity of pathological species of α-synuclein. In addition, cytokine release might affect α-synuclein in nearby cells in a similar manner, thus facilitating the selective spread and propagation of α-synuclein pathology in vulnerable cell populations. This vicious cycle could explain why α-synuclein pathology developed in implanted dopamine neurons in Parkinson's disease patients, how templating occurs in Parkinson's disease, and how toxic cytokines may be involved in the spread of α-synuclein pathology.

pathology (Duda *et al.*, 2002; Hoenen *et al.*, 2016; Zhang *et al.*, 2017) (Fig. 6).

Despite evidence of robust inflammation and microglial activation in graft deposit sites in our transplanted patients from the earliest time points evaluated, α-synuclein pathology was only observed many years afterwards. This suggests that initially, cellular clearance mechanisms may have been sufficient to clear misfolded proteins and prevent aggregation. Alternatively, cytokines released from microglia may initially have been present at too low a concentration to cause the accumulation and aggregation of misfolded proteins. However, over time, clearance capacities may be overwhelmed causing the accumulation and aggregation of the α-synuclein protein. Further, the accumulation of aggregated α-synuclein could accelerate the process, as it has been shown to interfere with both proteasomal and lysosomal clearance mechanisms (Snyder *et al.*, 2003; Martinez-Vicente *et al.*, 2008; Choi *et al.*, 2015) and to promote the microglial inflammatory cascade (Hoenen *et al.*, 2016).

It is also interesting to speculate on whether a similar sequence of events, but with a different initiating factor, could account for a 'templating' phenomenon in Parkinson's disease and explain how aggregated α-synuclein could promote misfolding of the wild-type protein. Based on the observations in our present study, we propose that the following sequence of events might occur in Parkinson's disease (Fig. 6): (i) α-synuclein misfolds and accumulates (possibly due to genetic, toxic, inflammatory, or stochastic causes); (ii) misfolded α-synuclein is released from cells; (iii) extracellular α-synuclein is taken up by microglia; (iv) microglia become activated; (v) cytokines are released from activated microglia; (vi) cytokines cleave/truncate host α-synuclein; (vii) truncated α-synuclein misfolds and aggregates; and (viii) misfolded α-synuclein continues to accumulate.

Thus, a vicious cycle might occur in Parkinson's disease in which misfolded α-synuclein promotes misfolding of native α-synuclein ultimately leading to the development of Lewy pathology and neurodegeneration (Fig. 4). Indeed, there is evidence of inflammation in sporadic Parkinson's disease as well as in asymptomatic patients with incidental Lewy bodies (McGeer *et al.*, 1988; Münch *et al.*, 2000; Doorn *et al.*, 2014). Toxic cytokines generated from activated microglia could also extend to affect other vulnerable nerve cells and thus promote the spread of α-synuclein pathology. That native α-synuclein is critical for this templating phenomenon to occur is illustrated by the observation that α-synuclein fibrils do not induce Lewy pathology in α-synuclein null animals (Luk *et al.*, 2012).

The number of transplanted brains we have been able to study is limited, but they represent the largest number of brains that have been examined from patients who have undergone a transplant procedure to date. Unfortunately, the examinations we were able to perform were restricted by tissue availability, so we were not able to assess cytokines or other inflammatory markers. However, these cases are rare, and the material available provides a unique opportunity to examine the temporal relationship between

Downloaded from https://academic.oup.com/brain/article/142/6/1690/5485812 by guest on 20 April 2024

inflammation/microglial activation and α-synuclein pathology in Parkinson's disease patients. Our findings are also of potential clinical importance as they suggest that this mechanism could account for the templating phenomenon that underlies the prion phenomenon, and that interventions that prevent microglial activation or inhibit cytokines such as caspase-1 or calpains might prevent the continued production of misfolded protein, and act as disease-modifying agents in Parkinson's disease (Games *et al.*, 2014; Olanow and Kordower, 2017).

Funding

The experiments reported were funded from a grant to J.H.K. from the Parkinson's Foundation.

Competing interests

C.W.O. has no direct conflict of interest with the present study. He owns stock in Clintrex, a pharmaceutical advisory company. J.H.K., M.S., G.H. and Y.C. have no direct conflict of interest with the present study.

References

Angot E, Steiner JA, Lema Tomé CM, Ekström P, Mattsson B, Björklund A, et al. Alpha-synuclein cell-to-cell transfer and seeding in grafted dopaminergic neurons in vivo. PLoS One 2012; 7: 1–11.

Bassil F, Fernagut PO, Bezard E, Pruvost A, Leste-Lasserre T, Hoang QQ, et al. Reducing C-terminal truncation mitigates synucleinopathy and neurodegeneration in a transgenic model of multiple system atrophy. Proc Natl Acad Sci USA 2016; 113: 9593–8.

Bennett ML, Bennett FC, Liddelow SA, Ajami B, Zamanian JL, Fernhoff NB, et al. New tools for studying microglia in the mouse and human CNS. Proc Natl Acad Sci USA 2016; 113: E1738–46.

Choi YR, Kang SJ, Kim JM, Lee SJ, Jou I, Joe EH, et al. FcγRIIB mediates the inhibitory effect of aggregated α-synuclein on microglial phagocytosis. Neurobiol Dis 2015; 83: 90–9.

Chu Y, Kordower JH. Age-associated increases of alpha-synuclein in monkeys and humans are associated with nigrostriatal dopamine depletion: Is this the target for Parkinson's disease? Neurobiol Dis 2007; 25: 134–49.

Cosenza MA, Zhao M-L, Si Q, Lee SC. Human brain parenchymal microglia express CD14 and CD45 and are productively infected by HIV-1 in HIV-1 encephalitis. Brain Pathol 2002; 12: 4442–55.

Cosenza-Nashat MA, Kim MO, Zhao ML, Suh HS, Lee SC. CD45 isoform expression in microglia and inflammatory cells in HIV-1 encephalitis. Brain Pathol 2006; 16: 256–65.

David S, Kroner A. Repertoire of microglial and macrophage responses after spinal cord injury. Nat Rev Neurocsi 2011; 12: 388–99.

Doorn KJ, Moors T, Drukarch B, van de Berg WDj, Lucassen PJ, van Dam AM. Microglial phenotypes and toll-like receptor 2 in the substantia nigra and hippocampus of incidental Lewy body disease cases and Parkinson's disease patients. Acta Neuropathol Commun 2014; 2: 90.

Duda JE, Giasson BI, Mabon ME, Lee VM, Trojanowski JQ. Novel antibodies to synuclein show abundant striatal pathology in Lewy body diseases. Ann Neurol 2002; 52: 205–10.

Dudvarski SN, Teodorczyk M, Ploen R, Zipp F, Schmidt MHH. Microglia-blood vessel interactions: a double-edged sword in brain pathologies. Acta Neuropathol 2016; 131: 347–63.

Dufty BM, Warner LR, Hou ST, Jiang SX, Gomez-Isla T, Leenhouts KM, et al. Calpain-cleavage of alpha-synuclein: connecting proteolytic processing to disease-linked aggregation. Am J Pathol 2007; 170: 1725–38.

Dzamko N, Gysbers A, Perera G, Bahar A, Shankar A, Gao J, et al. Toll-like receptor 2 is increased in neurons in Parkinson's disease brain and may contribute to alpha-synuclein pathology. Acta Neuropathol 2017; 133: 303–19.

Freed CR, Greene PE, Breeze RE. Transplantation of embryonic dopamine neurons for severe Parkinson's disease. N Engl J Med 2001; 344: 710–19.

Games D, Valera E, Spencer B, Rockenstein E, Mante M, Adame A, et al. Reducing C-terminal-truncated alpha-synuclein by immunotherapy attenuates neurodegeneration and propagation in Parkinson's disease-like models. J Neurosci 2014; 34: 9441–54.

Hoenen C, Gustin A, Birck C, Kirchmeyer M, Beaume N, Felten P, et al. Alpha-synuclein proteins promote pro-inflammatory cascades in microglia: stronger effects of the A53T mutant. PLoS One 2016; 11: 1–24.

Kordower JH, Chu Y, Hauser RA, Freeman TB, Olanow CW. Parkinson's disease pathology in long-term embryonic nigral transplants in Parkinson's disease. Nat Med 2008a; 14: 504–6.

Kordower JH, Freeman TB, Snow BJ, Vingerhoets FJG, Mufson EJ, Sanberg PR, et al. Neuropathologic evidence of graft survival and striatal reinnervation after the transplantation of fetal mesencephalic tissue in a patient with Parkinson's disease. N Eng J Med 1995; 332: 1118–24.

Kordower JH, Rosenstein JM, Collier TM, Burke MA, Chen E-Y, Li JM, et al. Functional fetal nigral grafts in a patient with Parkinson's disease: chemoanatomic, quantatative, ultrastructural, and metabolic studies. J Comp Neurol 1996; 370: 203–30.

Kordower JH, Styren S, DeKosky ST, Olanow CW, Freeman TB. Fetal grafting for Parkinson's disease: expression of immune markers in two patients with functional fetal nigral implants. Cell Transp 1997; 6: 213–9.

Kordower JH, Chu Y, Hauser RA, Olanow CW, Freeman TB. Transplanted dopaminergic neurons develop PD pathologic changes: a second case report. Mov Disord 2008b; 23: 2303–6.

Kordower JH, Dodiya HB, Kordower AM, Terpstra B, Paumier K, Madhavan L, et al. Transfer of host-derived α synuclein to grafted dopaminergic neurons in rat. Neurobiol Dis 2011; 43: 552–7.

Kordower JH, Goetz CG, Chu Y, Halliday GM, Nicholson DA, Musial TF, et al. Robust graft survival and normalized dopaminergic innervation do not obligate recovery in a Parkinson disease patient. Ann Neurol 2017; 81: 46–57.

Levesque S, Wilson B, Gregoria V, Thorpe LB, Dallas S, Polikov VS, et al. Reactive microgliosis: extracellular micro-calpain and microglia-mediated dopaminergic neurotoxicity. Brain 2010; 133: 808–21.

Li JY, Englund E, Holton JL, Soulet D, Hagell P, Lees AJ, et al. Lewy bodies in grafted neurons in subjects with Parkinson's disease suggest host-to-graft disease propagation. Nat Med 2008; 14: 501–3.

Li Q, Barres BA. Microglia and macrophages in brain homeostasis and disease. Nat Rev Immunol 2018; 18: 225–42.

Lopez-Atalaya JP, Askew KE, Sierra A, Gomez-Nicola D. Development and maintenance of the brain's immune toolkit: microglia and non-parenchymal brain macrophages. Dev Neurobiol 2018; 78: 561–79.

Luk KC, Kehm V, Carroll J, Zhang B, O'Brien P, Trojanowski JQ, et al. Pathological α-synuclein transmission initiates Parkinson-like neurodegeneration in nontransgenic mice. Science 2012; 338: 949–53.

Martinez-Vicente M, Talloczy Z, Kaushik S, Massey AC, Mazzulli J, Mosharov EV, et al. Dopamine-modified alpha-synuclein blocks chaperone-mediated autophagy. J Clin Invest 2008; 118: 777–88.

Downloaded from https://academic.oup.com/brain/article/142/6/1690/5485812 by guest on 20 April 2024

McGeer PL, Itagaki S, Boyes BE, McGeer EG. Reactive microglia are positive for HLA-DR in the substantia nigra of Parkinson's and Alzheimer's disease brains. Neurology 1988; 38: 1285–6.

Münch G, Lüth HJ, Wong A, Arendt T, Hirsch E, Ravid R, et al. Crosslinking of alpha-synuclein by advanced glycation endproducts—an early pathophysiological step in Lewy body formation? J Chem Neuroanat 2000; 20: 253–7.

Olanow CW. Goetz CG, Kordower JH, Stoessl J, Sossi V, Brin MF, et al. A double blind controlled trial of bilateral fetal nigral transplantation in Parkinson's disease. Ann Neurol 2003; 54: 403–14.

Olanow CW, Gracies J-M, Goetz CC, Stoessl AJ, Freeman T, Kordower J, et al. Clinical pattern and risk factors for dyskinesias following fetal nigral transplantation in Parkinson's disease: a double-blind video-based analysis. Mov Disord 2009a; 24: 336–43.

Olanow CW, Kordower JH, Lang AE, Obeso JA. Dopaminergic transplantation for Parkinson's disease: current status and future prospects. Ann Neurol 2009b; 66: 591–6.

Olanow CW, Prusiner SB. Is Parkinson's disease a prion disorder. Proc Natl Acad Sci USA 2009; 106: 12571–2.

Olanow CW, Brundin P. Alpha synuclein, prions, and Parkinson's Disease. Mov Disord 2013; 28: 31–40.

Olanow CW, Kordower JH. Targeting alpha synuclein as a therapy for Parkinson's disease: the battle begins. Mov Disord 2017; 32: 203–7.

Polymeropoulos MH, Lavedan C, Leroy E, Ide SE, Dehejia A, Dutra A, et al. Mutation in the alpha-synuclein gene identified in families with Parkinson's disease. Science 1997; 276, 2045–7.

Sampson TR, Debelius JW, Thron T, Janssen S, Shastri GG, Ilhan ZE, et al. Gut microbiota regulate motor deficits and neuroinflammation in a model of Parkinson's disease. Cell 2016; 167: 1469–80.

Schmitz C, Hof PR. Design-based stereology in neuroscience. Neuroscience 2005; 130: 813–31.

Snyder H, Mensah K, Theisler C, Lee J, Matouschek A, Wolozin B. Aggregated and monomeric alpha-synuclein bind to the S6' proteasomal protein and inhibit proteasomal function. J Biol Chem 2003; 278: 11753–9.

Spillantini MG, Schmidt ML, Lee VM, Trojanowski JQ, Jakes R, Goedert M. Alpha-synuclein in Lewy bodies. Nature 1997; 388: 839–40.

Tomé CLM, Tyson T, Rey NL, Grathwohl S, Britschgi M, Brundin P. Inflammation and α-synuclein's prion-like behavior in Parkinson's disease—is there a link? Mol Neurobiol 2013; 47: 561–74.

Valdinocci D, Radford RA, Siow SM, Chung RS, Pountney DL. Potential modes of intercellular α-synuclein transmission. Int J Mol Sci 2017; 22; 18.

Wang W, Nguyen LT, Burlak C, Chegini F, Guo F, Chataway T, et al. Caspase-1 causes truncation and aggregation of the Parkinson's disease-associated protein α-synuclein. Proc Natl Acad Sci USA 2016; 113: 9587–92.

West MJ, Slomianka L, Gundersen HJ. Unbiased stereological estimation of the total number of neurons in thesubdivisions of the rat hippocampus using the optical fractionator. Anat Rec 1991; 231: 482–97.

Zhang QS, Heng Y, Yuan YH, Chen NH. Pathological α-synuclein exacerbates the progression of Parkinson's disease through microglial activation. Toxicol Lett 2017; 265: 30–7.

Downloaded from https://academic.oup.com/brain/article/142/6/1690/5485812 by guest on 20 April 2024